Sexual dimorphism in the distribution and density of regulatory interneurons in the striatum

Meghan Van Zandt[a,1], Deirdre Flanagan[b], Christopher Pittenger[a,c,d,e,f,2]

a. Department of Psychiatry, Yale University School of Medicine, New Haven, CT
b. Yale College, New Haven, CT
c. Yale Child Study Center, Yale University School of Medicine, New Haven, CT
d. Department of Psychology, Yale School of Arts and Sciences, New Haven, CT
e. Center for Brain and Mind Health, Yale University School of Medicine, New Haven, CT
f. Wu-Tsai Institute, Yale University, New Haven, CT

Corresponding Authors:

1. Meghan.vanzandt@yale.edu
2. Christopher.pittenger@yale.edu, Phone: (203)-974-7675
   34 Park Street, Room W306, New Haven, CT, 06519, USA

Dr. Meghan Van Zandt is handling publication correspondence and is the primary producer of data, Dr. Christopher Pittenger will handle all future correspondence following publication and should Dr. Van Zandt depart the Pittenger Lab.

Abstract

Dysfunction of the cortico-basal circuitry – including its primary input nucleus, the striatum – contributes to neuropsychiatric disorders, including autism and Tourette Syndrome (TS). These conditions show marked sexual dimorphism, occurring more often in males than in females. Regulatory interneurons, including cholinergic interneurons (CINs) and parvalbumin-expressing GABAergic fast spiking interneurons (FSIs), are implicated in human neuropsychiatric disorders such as TS, and ablation of these interneurons produces relevant behavioral pathology in male mice, but not in females. Here we investigate sexual dimorphism in the density and distribution of striatal interneurons, using stereological quantification of CINs, FSIs, and somatostatin-expressing (SOM) GABAergic interneurons in the dorsal and ventral striatum in male and female mice. Males have a higher density of CINs than females, specifically in the dorsal striatum; females have equal distribution between dorsal and ventral striatum. FSIs showed similar effects, with a greater dorsal-ventral density gradient in males than in females. SOM interneurons were denser in the ventral than in the dorsal striatum, with no sexual dimorphism. These sex differences in the density and distribution of FSIs and CINs suggest a potential source of the sexual dimorphism seen in TS and autism spectrum disorder.

Keywords: Sex Differences, Parvalbumin, GABAergic, Cholinergic, Basal Ganglia

Introduction

The cortico-basal circuitry, particularly the striatum (caudate and putamen), is a locus of pathology in numerous neuropsychiatric disorders, including autism and Tourette's Syndrome (TS) (Swerdlow and Koob, 1987; Macpherson and Hikida, 2019; Chen et al., 2022). The striatum is the primary input nucleus and a central hub of the basal ganglia circuitry; it is implicated in numerous neural processes, including motion, effort, habit formation, motivation, and social behavior (Graybiel et al., 1994; Pennartz et al., 2009; Graybiel and Grafton, 2015; Bamford and Bamford, 2019; Suzuki et al., 2021).

The striatum is composed of GABAergic medium spiny neurons (MSNs, comprising ~95% of the neurons in the striatum in rodents)(Gerfen and Wilson, 1996) alongside several populations of regulatory interneurons, including ChAT-expressing cholinergic interneurons (CINs) and multiple subtypes of GABAergic interneurons, typically identified by their expression of markers such as parvalbumin (PV) and somatostatin (SOM) (Kawaguchi et al., 1995; Kawaguchi, 1997; Marin et al., 2000; Muñoz-Manchado et al., 2018). CINs innervate various GABAergic interneurons, including PV-expressing fast-spiking interneurons (FSIs) (Chang and Kita, 1992; Kocaturk et al., 2022), reciprocally regulate dopamine release

(Yorgason et al., 2017; Howe et al., 2019; Chantranupong et al., 2023), and can regulate excitatory glutamatergic input to MSNs (Pakhotin and Bracci, 2007; Ian Antón and Jun, 2011). FSIs are important regulators responsible for fine tuning MSN firing (Bennett and Bolam, 1994; Orduz et al., 2013) and integrate with other interneurons in coordinating movement bouts (Gritton et al., 2019) and regulating behavior (Lee et al., 2017). SOM interneurons play a complex role in regulating MSNs, FSIs, and CINs (Momiyama and Zaborszky, 2006; Cattaneo et al., 2019) and interact with dopaminergic afferents (Hathway et al., 1999; Gazan et al., 2020). Despite being a small percentage of striatal neurons, these interneurons critically regulate striatal function and behavioral output.

In alignment with this important functional role, interneuron pathology has been implicated in numerous neuropsychiatric disorders (Kataoka et al., 2010; Rapanelli et al., 2017a; Poppi et al., 2021; Brady et al., 2022). Deficits in cholinergic function are implicated in Parkinson's, Huntington's, and Alzheimer's Diseases, schizophrenia, bipolar disorder, and attention deficit-hyperactivity disorder (Lim et al., 2014). Postmortem studies in human patients with TS have shown significant reductions in striatal cholinergic (CINs) and parvalbumin-expressing (PV) GABAergic interneurons (Kalanithi et al., 2005; Kataoka et al., 2010; Lennington et al., 2016).

TS is diagnosed approximately twice as often in males as in females (Martino et al., 2013; Scahill et al., 2014). Whether striatal interneuron pathology in TS is similarly sexually dimorphic is unknown, but preclinical evidence is beginning to suggest that it may be. The striatal circuitry can be impacted by the estrous cycle (Cao et al., 2018; Zachry et al., 2021); both GABAergic and cholinergic interneurons express estrogen receptors (Almey et al., 2012; Almey et al., 2016). Furthermore, depletion of CINs during development (Cadeddu et al, 2023), or conjoint depletion of both CINs and FSIs in adults (Rapanelli et al., 2017b), produces dysregulated striatal activity and behavioral abnormalities of potential relevance to TS and related conditions – repetitive behavioral pathology, anxiety, and social deficits – in male mice, but not in females. This suggests an underlying sexual dimorphism in striatal interneurons, their regulation of local microcircuits, and their role in the modulation of striatum-dependent behaviors.

Here, using mice as a model system, we provide the first rigorous stereological comparison between males and females of the density and distribution of three different subtypes of striatal interneurons implicated in striatal function and in neuropsychiatric disease: PV- and SOM-expressing GABAergic interneurons and CINs.

Experimental Procedures

78 *Experimental Design*

79 All animal use followed protocols approved by Yale's Institutional Animal Care and Use Committee. Adult
80 male and female wild-type C57BL/6 mice (10-14 weeks old) were group housed in our animal facility in
81 self-ventilating cages, maintained on a 12hr light/dark cycle, and provided with food and water *ad libitium*.

82 For histology, mice were anesthetized (ketamine 100mg/kg and xylazine 10mg/kg, followed by isoflurane
83 inhalation until no response to noxious stimulus) followed by transcardial perfusion with 4%
84 paraformaldehyde in phosphate buffered saline (PBS) (Thermo Fisher) and brain extraction. Cryostat
85 sections were cut at 30 µm and mounted on Diamond White Glass Slides (Globe). For immunostaining for
86 identification and counting of interneurons, slides were incubated overnight at room temperature with
87 primary antibodies diluted in 0.1 M PBS containing 10% normal goat serum (Vector Labs) and 1% Triton-X
88 100 (AmericanBio). Primary antibodies were used as follows: Rabbit recombinant monoclonal anti-
89 somatostatin (1:250, Abcam, ab111912), mouse monoclonal anti-ChAT (1:250, Thermo Fisher, MA5-
90 31383), rabbit polyclonal anti-PV (1:250, Abcam, ab11427). Detection was performed with appropriate
91 secondary antibodies: polyclonal goat anti-rabbit coupled to Alexa Fluor 488 (1:1000, Thermo Fisher, A-
92 11008), polyclonal goat anti-rabbit coupled to Alexa Fluor 568 (1:1000, Thermo Fisher, A-11011),
93 recombinant polyclonal goat anti-mouse coupled to Alexa Fluor 488 (Thermo Fisher, A-28175), and
94 polyclonal goat anti-mouse coupled to Alexa Fluor 568 (1:1000, Thermo Fisher, A-11004). Sections were
95 then mounted and coverslipped in ProLong Gold with DAPI (Life Technologies).

96 Immunostained coronal striatal sections (30 µm, bregma 1.1mm-0.26mm) were visualized on a Zeiss
97 Scope.A1 using a Plan-APOCHROMAT 10x objective and an Axiocam 503 Mono at 100x magnification.
98 Microscope fields were systematically tiled over the entire dorsal and ventral striatum and stitched
99 together using the stitching plugin in FIJI (Schindelin et al., 2012) to provide a high-resolution image
100 throughout the extent of the structure. Only undamaged sections with consistent immunostaining
101 through the full extent of the striatum were included in analysis.

102 Whole striatum reconstructions were imported into StereoInvestigator 10 (MBF Biosciences) and regions
103 of interest were defined. For whole striatal analyses, the entire anatomical area of the striatum contained
104 in the image, bounded by the internal capsule/corpus callosum white matter and other landmarks
105 following the atlas of Paxinos (Franklin and Paxinos, 1997), was selected for quantification. For
106 dorsal/ventral subregion analyses we initially opted for an arbitrary division, since it is not clear *a priori*
107 what the meaningful subregions for quantification would be. The striatum was divided in half by a

horizontal line placed halfway between the dorsal and ventral extent of the structure (see Figures 1A, 2A, 3A). Neurons were counted using the fractionator tool in StereoInvestigator using a counting box size of 100 x 100 µm, excluding all neurons on the dashed bounding line. Data collected from left and right striatum were averaged. Following dorsal/ventral analysis, we then analyzed striatal interneuron density in the Caudate Putamen (CPu) and Nucleus Accumbens (Nacc) subregions, identified by alignment with the atlas of Paxinos (Franklin and Paxinos, 1997) and then counted using StereoInvestigator as described above. In total, 22 male and 17 female brains were analyzed, with two randomly selected sections per animal from within the range specified above.

Statistics

All data were imported into JASP Statistical Software (Eric-Jan Wagenmakers, University of Amsterdam) for statistical analysis. Data was tested for normality using the D'Agostino & Pearson test and outliers were excluded. For direct comparisons between sexes for whole striatum and to compare ratios of dorsal to ventral interneurons, a two-tailed unpaired t-test was performed. To compare between sexes for the dorsal and ventral sub-regions of the striatum, a two-way repeated-measures ANOVA was used, followed by Fisher's LSD post-hoc test (Table One). Graphs were generated using GraphPad Prism 10 (Graph Pad Software, LLC). Whiskers on bar and whisker plots indicate the min and max values, with all data points represented on graphs.

Results

We first quantified CIN density in male and female mice (Figure 1A-B). Male mice had a significantly higher density of ChAT+ interneurons (Figure 1B; two-tailed t-test, $t[26] = 2.305$, $p=0.031$). Males and females showed different patterns of CIN density in dorsal and ventral striatum (Figure 1C; 2way ANOVA: subregion x sex interaction: $F[1.00, 8.00] = 5.84$, $p = 0.042$). The density of ChAT interneurons in the female striatum was equal between the dorsal and ventral regions (Fisher's LSD: $p=0.43$). In contrast, males showed significantly higher density of ChAT+ neurons in the dorsal region compared to the ventral region (Fisher's LSD: $p=0.001$). The higher CIN density in males was restricted to the dorsal striatum (male vs female Fisher's LSD: $p = 0.03$); there was no difference between males and females in the ventral striatum ($p=0.53$). Analyzing the ratio of dorsal to ventral ChAT+ interneurons directly also showed higher ratios in males (1.55 ± 0.13) than in females (1.04 ± 0.022)(two-tailed t-test, $t[29] = 3.670$, $p=0.001$).

Quantification of CIN density in anatomically defined subregions, the CPu and Nacc, showed similar effects (Figure 1E). There were significant effects of both sex (Figure 1F; 2way ANOVA: $F[1.00, 16.00] = 4.769$, p =

138 0.044) and subregion (F[1.00, 16.00] = 5.991, p=0.026), with no interaction (sex x subregion F[1.00, 8.00]
139 = 0.614, p=0.456). There was a significantly higher density of ChAT+ interneurons in the CPu compared to
140 the NAcc in males (Fisher's LSD: p=0.037) but not in females (p=0.236).

141 Quantification of overall density of PV+ interneurons in whole striatum (Figure 2A-B) did not reveal
142 significant differences in density between males and females (Figure 2D; t-test, t[36] = 0.595; p=0.56).
143 However, analyzing across dorsal and ventral subregions uncovered sexually dimorphic effects (Figure 2C;
144 2-way ANOVA, sub-region x sex: F[1,11] = 6.94, p=0.012). In males, PV+ interneuron density was
145 significantly higher in the dorsal than in the ventral striatum (Fisher's LSD: p<0.001). In females, there was
146 a trend in the same direction, but it did not reach statistical significance (Fisher's LSD: p=0.07)(Figure 2D).
147 Analyzing the ratio of dorsal to ventral PV+ interneurons directly also showed higher ratios in males (1.57
148 ± 0.12) than in females (1.18 ± 0.06)(two-tailed t-test, t[36] = 2.769, p=0.009).

149 Quantification of PV+ interneurons by anatomical subregion (Figure 2E) also revealed significant sex
150 differences, with a significant effect of subregion (Figure 2F; Two-way ANOVA: F(1.00, 16.00) = 51.62,
151 p<0.001) and a significant interaction between sex and subregion (F[1.00, 10.00] = 9.477, p=0.012). Both
152 sexes showed significantly higher density of PV+ interneurons in the CPu compared to the NAcc (Fisher's
153 LSD: males p<0.001, females p=0.0013); males showed a significantly higher density of PV+ interneurons
154 in the CPu compared to females (p=0.012).

155 SOM+ interneuron densities across the full striatum did not differ between males and females (Figure 3A-
156 B; t-Test: t[27] = 0.515, p=0.61). Comparing dorsal and ventral striatum revealed higher density of SOM+
157 cells in the ventral than in the dorsal striatum in both males and females (Figure 3C-D; 2-way ANOVA,
158 subregion: F[1,15] = 9.96, p = 0.006), but no effect of sex or interaction. Both males and females showed
159 dorsal/ventral ratios below 1 (0.91 ± 0.05 and 0.90 ± 0.06, respectively; two-tailed t-test, t[27] = 0.08,
160 p=0.93). Quantification of SOM+ interneurons by anatomical subregion (Figure 3E) showed a significant
161 effect of subregion (Figure 3F; Two-way ANOVA: F[1.00, 12.00] = 27.45, p<0.001), but no effect of sex or
162 subregion x sex interaction. Both males (Fisher's LSD: p=0.001) and females (p=0.001) showed significantly
163 denser SOM+ interneurons in the NAcc compared to the CPu.

164 **Discussion**

165 Interneurons of the striatum are critical to basal ganglia function (Kreitzer, 2009) and have emerged as a
166 locus of pathology in a number of neuropsychiatric conditions (Rapanelli et al., 2017a; Poppi et al., 2021).
167 Biological sex modulates basal ganglia structure and function (Giedd et al., 1997; Rijpkema et al., 2012),

168 and numerous studies show sexual dimorphism in conditions in which basal ganglia dysregulation is
169 implicated, including TS (Martino et al., 2013; Scahill et al., 2014) and autism (Loomes et al., 2017).
170 However, no studies to date have systematically examined sexual dimorphism in the structure and function
171 of striatal interneurons.

172 Several populations of striatal interneuron have been found to be reduced in number in post-mortem
173 studies of individuals with persistent adult TS (Kalanithi et al., 2005; Kataoka et al., 2010; Lennington et al.,
174 2016); these studies included both male and female subjects but were not designed to detect sexually
175 dimorphic effects. In mice, we have found experimental depletion of cholinergic interneurons (CINs),
176 parvalbumin-expressing fast-spiking interneurons (FSIs), or both to destabilize the striatum, resulting in
177 repetitive behavioral pathology, social deficits, and other behavioral abnormalities (Xu et al, 2015; Xu et
178 al, 2016; Rapanelli et al, 2017; Cadeddu et al, 2023). Interestingly, these effects are sexually dimorphic,
179 appearing in male but not female mice, despite equivalent levels of interneuron depletion (Rapanelli et al,
180 2017; Cadeddu et al, 2023). The underlying differences in striatal anatomy or function that lead to this
181 differential susceptibility remain unclear.

182 Here, we document intriguing differences between male and female adult mice in striatal interneuron
183 density and distribution. Differential density and distribution of interneurons suggests differences in
184 striatal function, and perhaps in resilience and vulnerability to pathophysiological processes.

185 Cholinergic interneurons (CINs) play a central role in the striatal microcircuitry. CINs regulate the release
186 of both dopamine (Cachope et al., 2012; Threlfell et al., 2012) and GABA (Nelson et al., 2014) from
187 dopaminergic afferents from the substantia nigra. They also modulate multiple populations of GABAergic
188 interneurons, as well as MSNs (Poppi et al., 2021). We find a significant difference between sexes in both
189 density and distribution of these interneurons: The density of CINs is significantly higher in the dorsal
190 striatum in males than in females. This matches observations in our previous studies, in which a higher
191 density of these interneurons was observed in males than in females (Rapanelli et al, 2017; Cadeddu et al,
192 2023); however, these previous observations were incidental, without the rigorous quantification applied
193 here. While female mice have relatively even distribution of ChAT+ interneurons between the dorsal and
194 ventral striatum, males a greater density in the dorsal compared to the ventral area.

195 The presence of more CINs in the dorsal striatum and CPu of males than of females is perhaps surprising,
196 as our previous work shows that males are more sensitive to disruption of these cells (Rapanelli et al,
197 2017; Cadeddu et al, 2023). It might have been expected that a higher basal density of CINs would render

198 males more resilient to CIN depletion. The current data suggest a different model, that the dorsal
199 regulatory circuitry in males may be more reliant on CINs than that of females and thus is less able to
200 accommodate pathological CIN disruption.

201 PV-expressing FSIs are highly active interneurons innervating a wide variety of targets in the striatum
202 through both inhibition and disinhibition circuits (Duhne et al., 2021), and are particularly important in
203 regulating MSNs through feedforward inhibition (Koós and Tepper, 1999; Gittis et al., 2010; Gittis et al.,
204 2011; Adler et al., 2013; Lee et al., 2017). We find effects of both biological sex and striatal subregion on
205 FSI density. Male mice again exhibit a significantly higher density in the dorsal striatum than in the ventral
206 striatum; females also show a difference in density in the same direction, but it is less robust. Because FSIs
207 are an important source of inhibition in the striatum, this may suggest that the male and female striatum
208 differ in their excitatory-inhibitory balance. We have previously found depletion of FSIs in the dorsal
209 striatum to produce both repetitive behavioral pathology and elevated anxiety-like behavior (Xu et al,
210 2016), though it is not yet clear if these effects are specific to males. When both FSIs and CINs are depleted,
211 behavioral effects are seen only in males, suggesting that there may be a sex-specific effect (Rapanelli et
212 al., 2017b).

213 FSIs and CINs separately regulate MSN activity (Adler et al., 2013; Gritton et al., 2019), and each other
214 (Chang and Kita, 1992; DeBoer and Westerink, 1994; Faust et al., 2016). Sexual dimorphism in density and
215 distribution follows the same general pattern for both interneuron types, with higher density in the dorsal
216 CPu region of the striatum and a greater dorsal-ventral gradient towards the NAcc in males than in females
217 in both cases. This may suggest a single developmental process underlying both effects.

218 We found no sex differences in the density or distribution of SOM-expressing GABAergic interneurons.
219 However, both males and females had more SOM-expressing interneurons in the ventral compared to the
220 dorsal striatum. This pattern, quite distinct from that seen in CIN and FSI distribution, indicates that the
221 sexual dimorphism is not uniform across all components of the striatal microcircuitry but rather
222 differentially affects different cells and processes. This reinforces the idea that differential density,
223 distribution, and function of interneurons in males and females leads to distinct regional differences in
224 information processing in the basal ganglia circuitry.

225 In sum, we find consistent sex differences in the density and distribution of striatal interneurons, with a
226 higher density of both CINs and FSIs in the dorsal striatum, as well as differences in interneuron density
227 between dorsal and ventral striatum, more prominently in males. The mechanisms underlying these

differential patterns of interneuron density and distribution remain to be elucidated but are likely to involve sexually dimorphic modulation of developmental processes. Of note, estrogen receptors are expressed on both cholinergic (Almey et al., 2012) and GABAergic interneurons (Almey et al., 2016), providing a potential mechanism for sex hormones to regulate interneuron function. These findings represent a starting point for future work analyzing the impact of these differences on sexual dimorphism in both normal basal ganglia function and in the pathophysiology of a range of neuropsychiatric conditions, such as TS and ASD.

Acknowledgements

The authors thank Betsy D'Amico and the staff of the Yale Animal Resource Core and Charles River Laboratories for animal husbandry.

Funding sources

This work was supported by the grants F32MH123088 (MVZ), K24MH121571 (CP), and R01MH127259 (CP). This work was also supported by the State of Connecticut through its support of the Abraham Ribicoff Research Facilities at the Connecticut Mental Health Center; the reported work represents the views of the authors and not of the State of Connecticut.

Conflict of Interest

M. Van Zandt and D. Flanagan declare no competing financial interests. C Pittenger has consulted in the past year for Biohaven Pharmaceuticals, Freedom Biosciences, Ceruvia Life Sciences, Nobilis Therapeutics, Transcend Therapeutics, and F-Prime Capital Partners and has received research support from Biohaven, Freedom, and Transcend; none of these relationships are related to the current work. Dr. Pittenger holds equity in Alco Therapeutics and has pending patents related to the treatment of OCD, the actions of psychedelic drugs, and the role of specific antibodies in neuroimmune pathophysiology; again, none of these relationships are related to the current work.

References

Adler A, Katabi S, Finkes I, Prut Y, Bergman H (2013) Different correlation patterns of cholinergic and GABAergic interneurons with striatal projection neurons. Frontiers in Systems Neuroscience 7.

Almey A, Milner TA, Brake WG (2016) Estrogen receptor α and G-protein coupled estrogen receptor 1 are localized to GABAergic neurons in the dorsal striatum. Neuroscience Letters 622:118--123.

256 Almey A, Filardo EJ, Milner TA, Brake WG (2012) Estrogen receptors are found in glia and at extranuclear
257 neuronal sites in the dorsal striatum of female rats: evidence for cholinergic but not dopaminergic
258 colocalization. Endocrinology 153:5373-5383.
259 Bamford IJ, Bamford NS (2019) The Striatum's Role in Executing Rational and Irrational Economic Behaviors.
260 The Neuroscientist 25:475-490.
261 Bennett BD, Bolam JP (1994) Synaptic input and output of parvalbumin-immunoreactive neurons in the
262 neostriatum of the rat. Neuroscience 62:707-719.
263 Brady MV, Mariani J, Koca Y, Szekely A, King RA, Bloch MH, Landeros-Weisenberger A, Leckman JF,
264 Vaccarino FM (2022) Mispatterning and interneuron deficit in Tourette Syndrome basal ganglia
265 organoids. Molecular Psychiatry 27:5007-5019.
266 Cachope R, Mateo Y, Mathur BN, Irving J, Wang HL, Morales M, Lovinger DM, Cheer JF (2012) Selective
267 activation of cholinergic interneurons enhances accumbal phasic dopamine release: setting the
268 tone for reward processing. Cell Rep 2:33-41.
269 Cao J, Willett JA, Dorris DM, Meitzen J (2018) Sex Differences in Medium Spiny Neuron Excitability and
270 Glutamatergic Synaptic Input: Heterogeneity Across Striatal Regions and Evidence for Estradiol-
271 Dependent Sexual Differentiation. Frontiers in Endocrinology 9:173.
272 Cattaneo S, Zaghi M, Maddalena R, Bedogni F, Sessa A, Taverna S (2019) Somatostatin-Expressing
273 Interneurons Co-Release GABA and Glutamate onto Different Postsynaptic Targets in the Striatum.
274 bioRxiv:566984.
275 Chang HT, Kita H (1992) Interneurons in the rat striatum: relationships between parvalbumin neurons and
276 cholinergic neurons. Brain Research 574:307-311.
277 Chantranupong L, Beron CC, Zimmer JA, Wen MJ, Wang W, Sabatini BL (2023) Dopamine and glutamate
278 regulate striatal acetylcholine in decision-making. Nature 621:577-585.
279 Chen J, Tian C, Zhang Q, Xiang H, Wang R, Hu X, Zeng X (2022) Changes in Volume of Subregions Within
280 Basal Ganglia in Obsessive–Compulsive Disorder: A Study With Atlas-Based and VBM Methods.
281 Frontiers in Neuroscience 16.
282 DeBoer P, Westerink BHC (1994) GABAergic Modulation of Striatal Cholinergic Interneurons: An In Vivo
283 Microdialysis Study. Journal of Neurochemistry 62:70-75.
284 Duhne M, Lara-González E, Laville A, Padilla-Orozco M, Ávila-Cascajares F, Arias-García M, Galarraga E,
285 Bargas J (2021) Activation of parvalbumin-expressing neurons reconfigures neuronal ensembles in
286 murine striatal microcircuits. European Journal of Neuroscience 53:2149-2164.

Faust TW, Assous M, Tepper JM, Koós T (2016) Neostriatal GABAergic Interneurons Mediate Cholinergic Inhibition of Spiny Projection Neurons. The Journal of Neuroscience 36:9505-9511.

Franklin KBJ, Paxinos G (1997) The mouse brain in stereotaxic coordinates. San Diego: Academic Press San Diego.

Gazan A, Rial D, Schiffmann SN (2020) Ablation of striatal somatostatin interneurons affects MSN morphology and electrophysiological properties, and increases cocaine-induced hyperlocomotion in mice. Eur J Neurosci 51:1388-1402.

Gerfen CR, Wilson CJ (1996) Chapter II The basal ganglia. In: Handbook of chemical neuroanatomy, pp 371-468: Elsevier.

Giedd JN, Castellanos FX, Rajapakse JC, Vaituzis AC, Rapoport JL (1997) Sexual dimorphism of the developing human brain. Prog Neuropsychopharmacol Biol Psychiatry 21:1185-1201.

Gittis AH, Nelson AB, Thwin MT, Palop JJ, Kreitzer AC (2010) Distinct roles of GABAergic interneurons in the regulation of striatal output pathways. J Neurosci 30:2223-2234.

Gittis AH, Leventhal DK, Fensterheim BA, Pettibone JR, Berke JD, Kreitzer AC (2011) Selective inhibition of striatal fast-spiking interneurons causes dyskinesias. J Neurosci 31:15727-15731.

Graybiel AM, Grafton ST (2015) The striatum: where skills and habits meet. Cold Spring Harb Perspect Biol 7:a021691.

Graybiel AM, Aosaki T, Flaherty AW, Kimura M (1994) The Basal Ganglia and Adaptive Motor Control. Science 265:1826-1831.

Gritton HJ, Howe WM, Romano MF, DiFeliceantonio AG, Kramer MA, Saligrama V, Bucklin ME, Zemel D, Han X (2019) Unique contributions of parvalbumin and cholinergic interneurons in organizing striatal networks during movement. Nature Neuroscience 22:586-597.

Hathway GJ, Humphrey PP, Kendrick KM (1999) Evidence that somatostatin sst2 receptors mediate striatal dopamine release. Br J Pharmacol 128:1346-1352.

Howe M, Ridouh I, Allegra Mascaro AL, Larios A, Azcorra M, Dombeck DA (2019) Coordination of rapid cholinergic and dopaminergic signaling in striatum during spontaneous movement. eLife 8:e44903 , citation = eLife 42019;44908 e44903.

Ian Antón O, Jun BD (2011) Cholinergic modulation of synaptic integration and dendritic excitability in the striatum. Current Opinion in Neurobiology 21:425-432.

Kalanithi PS, Zheng W, Kataoka Y, DiFiglia M, Grantz H, Saper CB, Schwartz ML, Leckman JF, Vaccarino FM (2005) Altered parvalbumin-positive neuron distribution in basal ganglia of individuals with Tourette syndrome. Proc Natl Acad Sci U S A 102:13307-13312.

319 Kataoka Y, Kalanithi PS, Grantz H, Schwartz ML, Saper C, Leckman JF, Vaccarino FM (2010) Decreased
320 number of parvalbumin and cholinergic interneurons in the striatum of individuals with Tourette
321 syndrome. J Comp Neurol 518:277-291.
322 Kawaguchi Y (1997) Neostriatal cell subtypes and their functional roles. Neurosci Res 27:1-8.
323 Kawaguchi Y, Wilson CJ, Augood SJ, Emson PC (1995) Striatal interneurones: chemical, physiological and
324 morphological characterization. Trends Neurosci 18:527-535.
325 Kocaturk S, Guven EB, Shah F, Tepper JM, Assous M (2022) Cholinergic control of striatal GABAergic
326 microcircuits. Cell Rep 41:111531.
327 Koós T, Tepper JM (1999) Inhibitory control of neostriatal projection neurons by GABAergic interneurons.
328 Nat Neurosci 2:467-472.
329 Kreitzer AC (2009) Physiology and pharmacology of striatal neurons. Annu Rev Neurosci 32:127-147.
330 Lee K, Holley SM, Shobe JL, Chong NC, Cepeda C, Levine MS, Masmanidis SC (2017) Parvalbumin
331 Interneurons Modulate Striatal Output and Enhance Performance during Associative Learning.
332 Neuron 93:1451-1463 e1454.
333 Lennington JB, Coppola G, Kataoka-Sasaki Y, Fernandez TV, Palejev D, Li Y, Huttner A, Pletikos M, Sestan N,
334 Leckman JF, Vaccarino FM (2016) Transcriptome Analysis of the Human Striatum in Tourette
335 Syndrome. Biol Psychiatry 79:372-382.
336 Lim SAO, Kang UJ, McGehee DS (2014) Striatal cholinergic interneuron regulation and circuit effects.
337 Frontiers in Synaptic Neuroscience 6.
338 Loomes R, Hull L, Mandy WPL (2017) What Is the Male-to-Female Ratio in Autism Spectrum Disorder? A
339 Systematic Review and Meta-Analysis. J Am Acad Child Adolesc Psychiatry 56:466-474.
340 Macpherson T, Hikida T (2019) Role of basal ganglia neurocircuitry in the pathology of psychiatric disorders.
341 Psychiatry and Clinical Neurosciences 73:289-301.
342 Marin O, Anderson SA, Rubenstein JL (2000) Origin and molecular specification of striatal interneurons. J
343 Neurosci 20:6063-6076.
344 Martino D, Macerollo A, Leckman JF (2013) Neuroendocrine aspects of Tourette syndrome. Int Rev
345 Neurobiol 112:239---279.
346 Momiyama T, Zaborszky L (2006) Somatostatin Presynaptically Inhibits Both GABA and Glutamate Release
347 Onto Rat Basal Forebrain Cholinergic Neurons. Journal of Neurophysiology 96:686-694.
348 Muñoz-Manchado AB, Gonzales CB, Zeisel A, Munguba H, Bekkouche B, Skene NG, Lönnerberg P, Ryge J,
349 Harris KD, Linnarsson S, Hjerling-Leffler J (2018) Diversity of Interneurons in the Dorsal Striatum
350 Revealed by Single-Cell RNA Sequencing and PatchSeq. Cell Reports 24:2179--2190.e2177.

Nelson AB, Hammack N, Yang CF, Shah NM, Seal RP, Kreitzer AC (2014) Striatal cholinergic interneurons Drive GABA release from dopamine terminals. Neuron 82:63-70.

Orduz D, Bischop DP, Schwaller B, Schiffmann SN, Gall D (2013) Parvalbumin tunes spike-timing and efferent short-term plasticity in striatal fast spiking interneurons. The Journal of Physiology 591:3215-3232.

Pakhotin P, Bracci E (2007) Cholinergic Interneurons Control the Excitatory Input to the Striatum. The Journal of Neuroscience 27:391-400.

Pennartz CMA, Berke JD, Graybiel AM, Ito R, Lansink CS, Meer Mvd, Redish AD, Smith KS, Voorn P (2009) Corticostriatal Interactions during Learning, Memory Processing, and Decision Making. The Journal of Neuroscience 29:12831-12838.

Poppi LA, Ho-Nguyen KT, Shi A, Daut CT, Tischfield MA (2021) Recurrent Implication of Striatal Cholinergic Interneurons in a Range of Neurodevelopmental, Neurodegenerative, and Neuropsychiatric Disorders. Cells 10.

Rapanelli M, Frick LR, Pittenger C (2017a) The Role of Interneurons in Autism and Tourette Syndrome. Trends Neurosci 40:397-407.

Rapanelli M, Frick LR, Xu M, Groman SM, Jindachomthong K, Tamamaki N, Tanahira C, Taylor JR, Pittenger C (2017b) Targeted Interneuron Depletion in the Dorsal Striatum Produces Autism-like Behavioral Abnormalities in Male but Not Female Mice. Biol Psychiatry 82:194-203.

Rijpkema M, Everaerd D, van der Pol C, Franke B, Tendolkar I, Fernández G (2012) Normal sexual dimorphism in the human basal ganglia. Hum Brain Mapp 33:1246-1252.

Scahill L, Specht M, Page C (2014) The Prevalence of Tic Disorders and Clinical Characteristics in Children. J Obsessive Compuls Relat Disord 3:394-400.

Schindelin J, Arganda-Carreras I, Frise E, Kaynig V, Longair M, Pietzsch T, Preibisch S, Rueden C, Saalfeld S, Schmid B, Tinevez J-Y, White DJ, Hartenstein V, Eliceiri K, Tomancak P, Cardona A (2012) Fiji: an open-source platform for biological-image analysis. Nature Methods 9:676-682.

Suzuki S, Lawlor VM, Cooper JA, Arulpragasam AR, Treadway MT (2021) Distinct regions of the striatum underlying effort, movement initiation and effort discounting. Nature Human Behaviour 5:378-388.

Swerdlow NR, Koob GF (1987) Dopamine, schizophrenia, mania, and depression: Toward a unified hypothesis of cortico-striatopallido-thalamic function. Behavioral and Brain Sciences 10:197--208.

Threlfell S, Lalic T, Platt NJ, Jennings KA, Deisseroth K, Cragg SJ (2012) Striatal dopamine release is triggered by synchronized activity in cholinergic interneurons. Neuron 75:58-64.

383 Yorgason JT, Zeppenfeld DM, Williams JT (2017) Cholinergic Interneurons Underlie Spontaneous Dopamine
384 Release in Nucleus Accumbens. J Neurosci 37:2086-2096.
385 Zachry JE, Nolan SO, Brady LJ, Kelly SJ, Siciliano CA, Calipari ES (2021) Sex differences in dopamine release
386 regulation in the striatum. Neuropsychopharmacology 46:491-499.

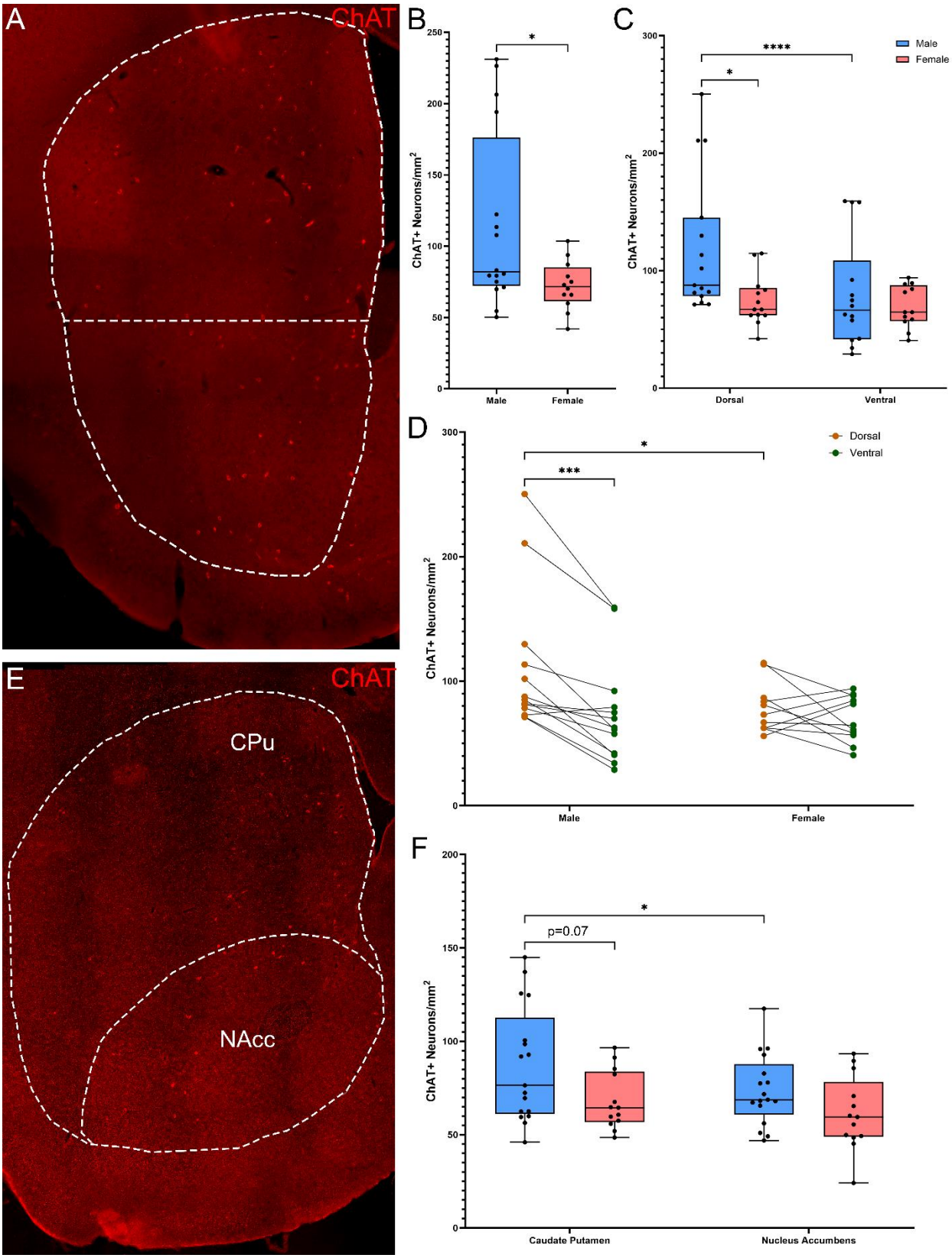
A
ChAT
B
C
D
E
ChAT
CPu
NAcc
F
ChAT+ Neurons/mm²
Male
Female
Dorsal
Ventral
Caudate Putamen
Nucleus Accumbens
p=0.07

387

Figure One. Cholinergic Interneurons are denser and show a dorsally skewed distribution in the striatum of male versus female mice. A. Representative whole striatum reconstruction of high-resolution microscope images of ChAT-expressing interneurons from a male mouse striatum. Dashed lines indicate counting regions for dorsal and ventral striatum. **B.** Stereological quantification of the density of ChAT+ interneurons per mm^2 over the whole mouse striatum showing a higher density of ChAT+ neurons in males compared to females (*Two-tailed t-test, t[26] = 2.305, p=0.029). **C.** Quantification of the density of ChAT+ interneurons divided over the dorsal and ventral sub-regions of the striatum reveals a significant effect of subregion (f[1.00, 14.00] = 10.42, p=0.006), a trend towards significant effect of sex (f[1,14] = 3.79, p=0.07), and a significant interaction of subregion and sex (2way ANOVA, f[1,8] = 5.55, p=0.046). ChAT+ interneurons in the male dorsal striatum were significantly denser than both female dorsal striatum (*Fisher's LSD, p=0.032) and male ventral striatum (**p=0.001). **D.** Alternative representation of the data from C, showing distribution gradients of ChAT+ interneurons by individual animal. **E.** Representative whole striatum reconstruction of high-resolution microscope images of ChAT-expressing interneurons, with dashed lines indicating counting regions for CPu and NAcc. **F.** Quantification of the density of ChAT+ interneurons divided over the CPu and NAcc sub-regions of the striatum reveals a significant effect of subregion (2way ANOVA, f[1,16] = 5.991, p=0.026) and sex (f[1,16] = 4.769, p=0.044); without interaction (f[1,8] = 0.614, p=0.456). Males showed significantly higher ChAT+ interneuron density in the CPu compared to the NAcc (*Fisher's LSD: p=0.037) while females did not (p=0.237) and there was a trend towards higher density of ChAT in the male CPu compared to the female CPu (p=0.07).

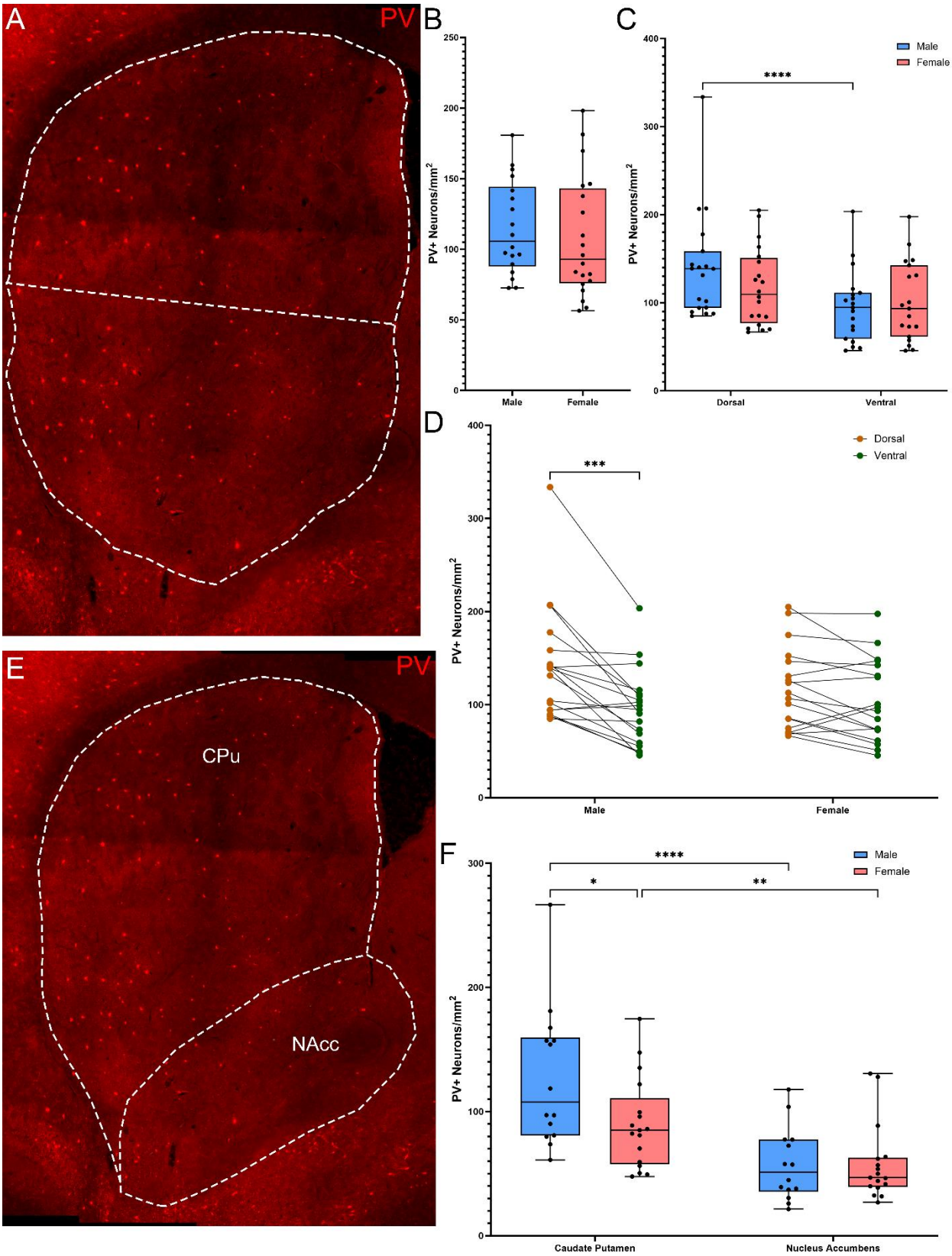
A
PV
B
PV+ Neurons/mm2
Male
Female
C
Male
Female
****
PV+ Neurons/mm2
Dorsal
Ventral
D
Dorsal
Ventral
***
PV+ Neurons/mm2
Male
Female
E
PV
CPu
NAcc
F
Male
Female
****
*
**
PV+ Neurons/mm2
Caudate Putamen
Nucleus Accumbens

407

408 **Figure Two. Parvalbumin-expressing interneurons are more concentrated in the dorsal versus the**
409 **ventral striatum in male, but not female mice. A.** Representative whole striatum reconstruction of high-
410 resolution microscope images of PV-expressing interneurons from a male mouse striatum. Dashed lines
411 indicate counting regions for dorsal and ventral striatum. **B.** Quantification of the density of PV+
412 interneurons per mm^2 over the whole mouse striatum using stereological methods shows similar densities
413 of PV+ neurons between sexes (Two-tailed t-test, t[36] = 0.595; p=0.56). **C.** Quantification of the density
414 of PV+ interneurons divided over the dorsal and ventral sub-regions of the striatum reveals a significant
415 effect of subregion (f[1,20] = 25.32), p<0.001) and a significant interaction of subregion x sex (2way ANOVA,
416 f[1,13] = 8.39, p=0.01). Males show a different distribution of PV+ interneurons than females, in that they
417 are significantly denser in the dorsal striatum (****Fisher's LSD, p<0.001), while females had a more equal
418 distribution between the dorsal and ventral regions (p=0.10). **D.** Alternative representation of the data
419 from C, showing distribution gradients of PV+ interneurons by individual animal. **E.** Representative whole
420 striatum reconstruction of high-resolution microscope images of PV-expressing interneurons, with dashed
421 lines indicating counting regions for CPu and NAcc. **F.** Quantification of the density of PV+ interneurons
422 divided over the CPu and NAcc sub-regions of the striatum reveals a significant effect of subregion (2way
423 ANOVA, f[1,16] = 51.62, p<0.001) and a significant interaction of sex and subregion (f[1,10] = 9, p=0.044).
424 Males showed significantly higher PV+ interneuron density in the CPu compared to the NAcc (****Fisher's
425 LSD: p<0.001) while females showed a similar, but less robust trend (***p=0.001). PV+ interneurons in the
426 CPu were significantly denser in males than in females (*p=0.012), but there were no differences in density
427 in the NAcc (p=0.96).

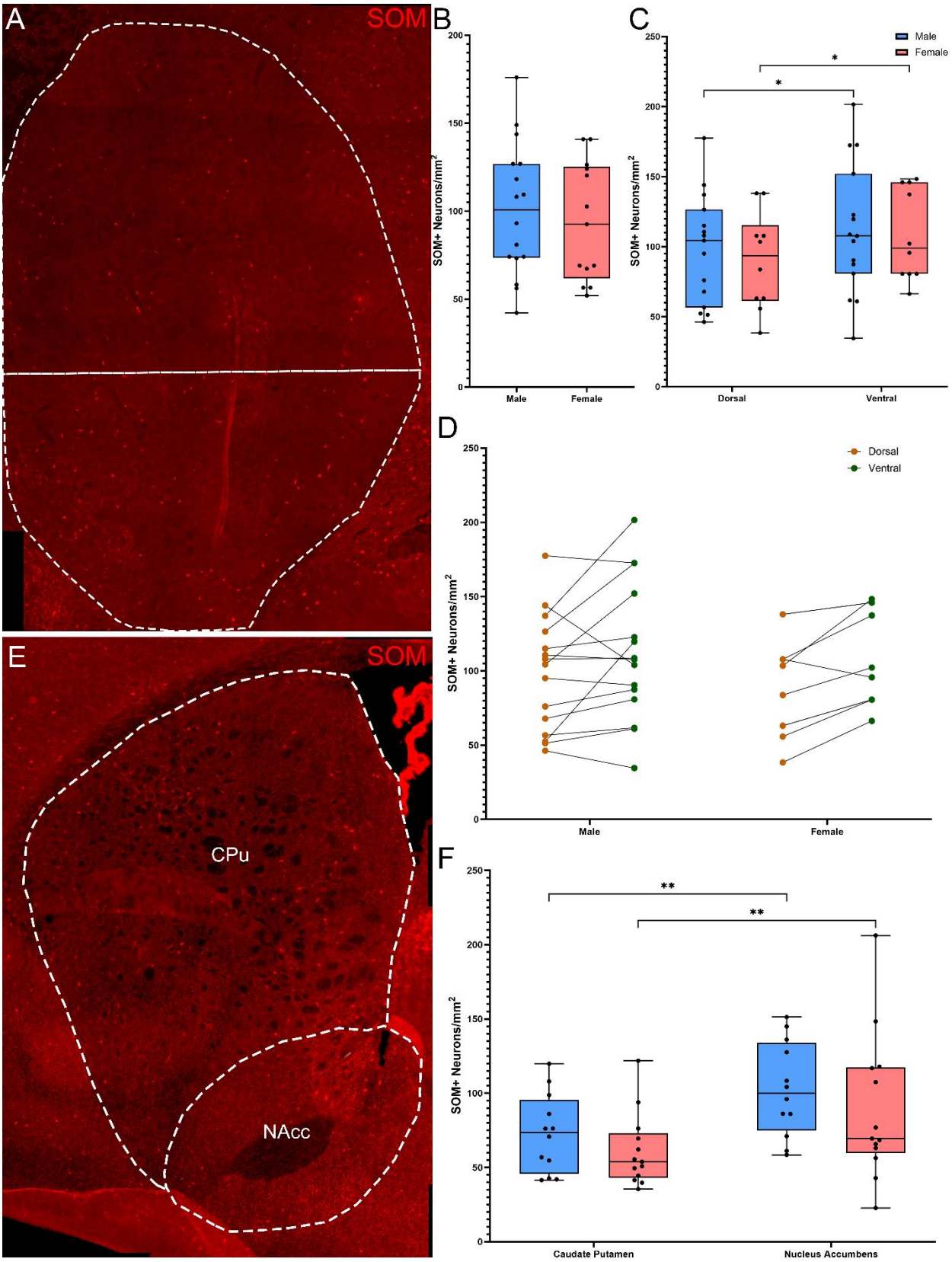
A
SOM
B
C
Male
Female
SOM+ Neurons/mm²
Male
Female
Dorsal
Ventral
D
Dorsal
Ventral
E
SOM
CPu
NAcc
F
Caudate Putamen
Nucleus Accumbens

428

429 **Figure Three. Somatostatin-expressing interneurons are denser in the ventral striatum in both male and**
430 **female mice. A.** Representative whole striatum reconstruction of high-resolution microscope images of
431 SOM-expressing interneurons from a male mouse striatum. **B.** Quantification of the density of SOM+
432 interneurons per mm^2 over the whole mouse striatum using stereological methods, showing similar
433 densities of SOM+ neurons between sexes (Two-tailed t-test, t[27] = 0.515, p=0.61). **E.** Quantification of
434 the density of SOM+ interneurons divided over the dorsal and ventral sub-regions of the striatum reveals
435 an effect of subregion (f[1,14] = 8.981, p=0.009) but no interaction with sex (f[1,10] = 0.20, p=0.677). Both
436 males (*Fisher's LSD, p=0.04) and females (*p=0.03) show slight but significantly higher densities of SOM
437 interneurons in the ventral compared to the dorsal striatum, but no differences between sexes in either
438 region. **D.** Alternative representation of the data from C, showing distribution gradients of SOM+
439 interneurons by individual animal. **E.** Representative whole striatum reconstruction of high-resolution
440 microscope images of SOM-expressing interneurons, with dashed lines indicating counting regions for CPu
441 and NAcc. **F.** Quantification of the density of SOM+ interneurons divided over the CPu and NAcc sub-
442 regions of the striatum reveals a significant effect of subregion (2way ANOVA, f[1,12] = 27.45, p<0.001)
443 and no effect of sex (f[1,12] = 1.308, p=0.275) or interaction (f[1,8] = 0.019, p=0.894). Both males and
444 females showed significantly higher SOM+ interneuron density in the NAcc compared to the CPu
445 (**Fisher's LSD: p=0.001 for both) with no sex differences in density for either the CPu (p=0.369) or the
446 NAcc (p=0.302).

447